International Journal of Scientific Research & Engineering Trends
Volume 12, Issue 5, Sep-Oct-2026, ISSN (Online): 2395-566X

NanoCircula-GW: A Nanomaterial-Enhanced Photocatalytic Oxidation and Mixed-Matrix Membrane Treatment Train with Nutrient Recovery for Circular Greywater Reuse

Dr. Muhammadu Sathik Raja[1],
Research Coordinator,
Dhanalakshmi Srinivasan Institute of Research and Technology[1].

Dr.Surya[2],
Associate Professor, Department of Biochemistry,
Dhanalakshmi Srinivasan Institute of Research and Technology[2].

Sudha Shiri J[3],
Assistant Professor, Department of Bio-Medical Engineering,
Dhanalakshmi Srinivasan Institute of Research and Technology[3]

Dr. Baskaran Nandhini[4],
Assistant Professor, Department of Biochemistry,
Dhanalakshmi Srinivasan Institute of Research and Technology[4].

Abstract — Conventional decentralised greywater units remove bulk organics but leave surfactants, micropollutants, pathogens and nutrients that restrict reuse and waste recoverable resources. This paper presents NanoCircula-GW, a circular treatment train that integrates an aerobic bio-reactor and sand–carbon filtration with a hydrothermally synthesised g-C3N4/TiO2 photocatalytic UV-AOP reactor, a phase-inversion PES membrane loaded with TiO2/ZrO2 nanoparticles, and a struvite crystallisation vessel for nitrogen and phosphorus recovery. A gradient-boosting surrogate model trained on operating records predicts photocatalytic removal and membrane flux decline and recommends catalyst loading, irradiation time and cleaning intervals. Using the PJ-NTP-2026 dataset from a 2 KLD pilot plant, the train achieved COD removal of 93.4%, surfactant removal of 97.8%, a flux recovery ratio of 94.1% and phosphate recovery of 86.5%, while the surrogate predicted removal efficiency with an R^2 of 0.94.

Keywords— Greywater reuse; Photocatalysis; g-C3N4/TiO2 heterojunction; Mixed-matrix membrane; Struvite recovery; Machine learning; Circular economy.

I. INTRODUCTION

Greywater accounts for the largest share of domestic wastewater by volume and carries a comparatively low pollutant load, which makes it the most practical stream for on-site recycling in institutions and housing. Its contaminant profile nonetheless includes surfactants, personal-care residues, pathogens and emerging micropollutants that present health risks when reuse is not preceded by adequate treatment [1]. Characterisation studies across different economies show that greywater composition depends strongly on its source and on living standards, and that no single treatment technology meets every reuse objective [2]. Biological units such as moving bed biofilm reactors remove much of the biodegradable organic matter and part of the nutrients in decentralised settings, yet their effluent often retains colour, recalcitrant organics and microbial risk [3].

Recent work on circular water management argues that wastewater systems should be judged not only by effluent quality but also by the resources they return to use [4], and that integrating treatment innovation with the recovery of water, energy and nutrients is now a central research direction [5]. Existing greywater studies, however, examine advanced oxidation, membranes or nutrient recovery in isolation, under laboratory conditions and without an intelligent layer that

© 2026 IJSRET

adapts operation to changing influent. A treatment train that combines these steps in one compact, data-guided unit has not been reported.

This work introduces NanoCircula-GW and makes four contributions. It develops a hydrothermally synthesised g-C3N4/TiO2 heterojunction photocatalyst immobilised in a UV-AOP reactor for surfactant and micropollutant degradation. It fabricates a low-cost PES membrane modified with TiO2/ZrO2 nanoparticles through phase inversion for antifouling polishing. It integrates a struvite crystallisation vessel that recovers nitrogen and phosphorus as a slow-release fertiliser. Finally, it couples these stages through a gradient-boosting surrogate model that predicts removal and fouling and recommends operating settings.

The overall objective is to convert a linear greywater stream into a circular one that returns safe non-potable water and agricultural nutrients from the same facility. The significance of the framework lies in demonstrating that nanomaterials fabricated with modest laboratory equipment, coupled with data-driven operation, can raise reuse quality while lowering chemical and cleaning demand for institutional and community-scale plants.

II. LITERATURE REVIEW

Membrane bioreactors remain the most established route to high-quality recycled greywater, with pre-treatment and post-disinfection identified as critical to controlling fouling and ensuring effluent safety [6]. Recent investigations have extended the assessment of these systems to emerging contaminants, showing that membrane bioreactors retain most microplastic fibres released from laundry greywater [7]. Hybrid hydrodynamic cavitation and Fenton oxidation has also been applied to domestic greywater, producing water suitable for irrigation and domestic non-potable uses [8]. These studies confirm the potential of advanced units but also highlight the energy and chemical demand that limits their adoption in small plants.

Ultraviolet-driven advanced oxidation is now accepted in potable reuse, and a recent review of UV–chlorine systems emphasised the influence of ammonia and chloramines on radical generation and the need to monitor transformation products [9]. Metal-free graphitic carbon nitride coupled with TiO2 improved charge separation and accelerated the decolourisation rate of an azo dye by about two and a half times relative to bare TiO2 [10]. A magnetically separable Fe3O4@TiO2/g-C3N4 heterostructure extended visible-light absorption and enabled catalyst recovery after tetracycline degradation [11]. Both studies point to heterojunction photocatalysts as promising polishing agents, although neither was tested on real greywater.

Mixed-matrix PES membranes containing TiO2/ZrO2 nanocomposites improved hydrophilicity, rejection and resistance to fouling for dye-laden water [12]. PES membranes doped with CuO and ZnO nanoparticles exhibited greater mechanical strength and higher removal of colour, organic carbon and metals during surface-water filtration [13]. A review of fouling modelling showed that artificial neural networks can predict flux decline and fouling resistance from feed and operating variables [14]. These results indicate that nanoparticle loading and predictive models can jointly address fouling, the main operating barrier of membrane polishing.

Artificial intelligence applied to membrane-based wastewater treatment has been reviewed with practical guidance on architecture, input selection and training for fouling prediction [15]. Ensemble learners trained on photocatalytic experiments with TiO2–lignin biochar composites predicted dye degradation efficiency and ranked catalyst dose and pollutant concentration as the dominant factors [16]. Extreme gradient boosting likewise outperformed the other algorithms tested in predicting the photocatalytic capacity of doped BiVO4 nanoparticles [17]. Such surrogates reduce experimental effort, but they have not yet been linked to an operating treatment train.

Struvite crystallisation has been reviewed as a mature route to recover nitrogen and phosphorus, with pH, magnesium ratio and supersaturation identified as the governing variables [18]. Adsorption and chemical precipitation have been compared for phosphate recovery, highlighting the effects of coexisting ions and adsorbent properties [19]. A further review of real-wastewater applications called for cost-efficient reactor designs and regulation-ready fertiliser products to move struvite from laboratory to market [20]. No reviewed study combines nanomaterial-based polishing, membrane separation and nutrient recovery with data-driven operation for greywater, which is the gap addressed by NanoCircula-GW.

III. METHODOLOGY

NanoCircula-GW is implemented within the 2 KLD circular water recycling pilot plant and its supporting laboratory. Greywater collected from campus sources passes through an equalisation tank, an aerobic bio-reactor and a sand–activated carbon filter before entering the nanomaterial-enhanced

© 2026 IJSRET

polishing stages. The UV-AOP reactor houses immobilised g-C3N4/TiO2 photocatalyst plates, the mixed-matrix membrane module removes residual particles and microorganisms, and a nutrient-rich side stream is directed to the struvite vessel. A surrogate model trained on plant and laboratory records predicts stage performance and recommends operating settings through a monitoring dashboard. Figure 1 illustrates the proposed architecture.

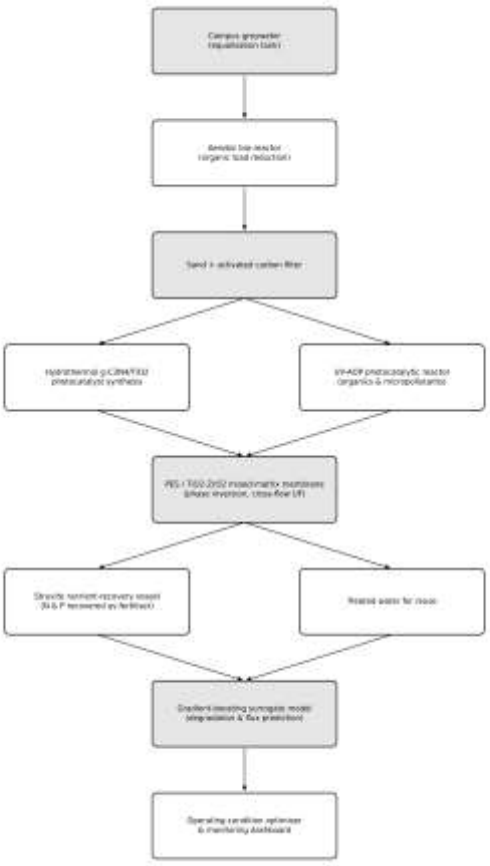

Figure 1: Proposed architecture of the NanoCircula-GW treatment train

1. Dataset Description and Preparation

The study uses the PUNARJAL Nano-Treatment Performance Dataset (PJ-NTP-2026), generated by the Smart Water Innovation Laboratory, [Institution Name], from the 2 KLD pilot plant and its bench-scale units, and archived at [dataset repository link / DOI]. Each record represents one treatment batch and contains influent and stage-wise effluent values of pH, turbidity, TDS, COD, BOD5, linear alkylbenzene sulphonate, total nitrogen, phosphate and E. coli, together with operating variables such as catalyst loading, irradiation time, UV intensity, transmembrane pressure, cross-flow velocity, magnesium-to-phosphate ratio and reaction pH. Analyses were performed with a UV–visible spectrophotometer, multiparameter analyser, COD digester, BOD incubator and membrane-filtration microbiology. Preparation included unit harmonisation, removal of batches with incomplete stage data, outlier screening against duplicate analyses and standardisation fitted on training data only.

2. Photocatalyst Synthesis and Characterisation

Graphitic carbon nitride is obtained by thermal polycondensation of melamine in the muffle furnace, and TiO2 nanoparticles are grown on the exfoliated sheets in Teflon-lined hydrothermal autoclaves. Composites with different g-C3N4 to TiO2 mass ratios are prepared to identify the most active heterojunction. The products are washed and separated in the refrigerated centrifuge, dried and calcined. Optical absorption and band-gap shifts are examined with the UV–visible spectrophotometer, while structural and surface characterisation is carried out at an external analytical facility. The optimised powder is immobilised on stainless-steel plates through a binder-assisted coating so that the catalyst remains inside the reactor and no nanoparticle separation step is needed after treatment.

3. Photocatalytic UV-AOP Reactor

The filtered effluent enters a recirculating reactor fitted with UV lamps and coated catalyst plates arranged parallel to the flow. Hydrogen peroxide dosing is available as an auxiliary oxidant for high-load batches. Batch experiments vary catalyst loading, irradiation time, initial pH and peroxide dose, and samples are taken at fixed intervals to determine COD, surfactant and colour removal and to derive apparent rate constants. Reusability is assessed by repeating degradation cycles with the same plates after rinsing, and scavenger tests with established radical quenchers identify the reactive species responsible for degradation. The optimised conditions are then transferred to continuous operation within the pilot plant, where the reactor treats the full filtered stream.

4. Mixed-Matrix Membrane Fabrication and Testing

Casting solutions are prepared by dissolving PES with a pore-forming additive in a polar aprotic solvent and dispersing TiO2/ZrO2 nanoparticles at low loading by sonication. Films are cast with the manual applicator and solidified in the phase-inversion bath. Pristine and modified membranes are evaluated in the lab-scale cross-flow flat-sheet cell for pure water flux, rejection of turbidity, organic matter and E. coli, and fouling

© 2026 IJSRET

behaviour during filtration of AOP-treated greywater. Flux recovery after hydraulic cleaning separates reversible from irreversible fouling. Contact-angle and porosity measurements support the interpretation of changes in permeability and antifouling behaviour, and the best-performing formulation is scaled to the pilot membrane module.

5. Struvite Nutrient Recovery

Concentrate from the membrane stage and nutrient-rich bio-reactor supernatant are combined in the recovery vessel, where magnesium is supplied as magnesium chloride and pH is raised with sodium hydroxide to induce struvite crystallisation. Mixing speed, reaction time, magnesium-to-phosphate molar ratio and pH are varied to determine the conditions that give the highest recovery with acceptable crystal size. Crystals are separated, dried at low temperature and examined for purity, while the supernatant is returned to the bio-reactor. The recovered product is evaluated as a slow-release fertiliser for campus landscaping, so that the nutrient loop is closed alongside the water loop within the same facility.

6. Surrogate Modelling and Operating Optimisation

A gradient-boosting regression model is trained on PJ-NTP-2026 to predict three targets: COD removal in the UV-AOP reactor, normalised flux after a filtration cycle and phosphate recovery in the struvite vessel. Random forest, support vector regression and artificial neural network models serve as baselines. Hyperparameters are tuned through cross-validation on the training portion, and Shapley additive explanations identify the operating variables that govern each target. The trained surrogate is coupled with a constrained search that recommends catalyst loading, irradiation time, cleaning interval and magnesium dose that meet reuse targets at minimum energy and chemical use. Recommendations are presented to operators on the monitoring dashboard.

IV. RESULTS AND DISCUSSION

Experimental work used the laboratory and pilot infrastructure of the PUNARJAL programme, comprising Teflon-lined hydrothermal autoclaves, a muffle furnace rated to 1100 °C, a high-speed refrigerated centrifuge, a manual film applicator with phase-inversion bath, a lab-scale cross-flow flat-sheet test cell, a double-beam UV–visible spectrophotometer, a multiparameter water-quality analyser with COD digester and BOD incubator, membrane-filtration microbiology equipment and the 2 KLD pilot plant with its UV-AOP unit and nutrient-recovery vessel. Modelling was performed on a GPU workstation with an Intel Xeon W-2245 processor, 64 GB RAM, an NVIDIA RTX-class GPU with 24 GB memory and 4 TB solid-state storage running Ubuntu 22.04 LTS, using Python with scikit-learn, XGBoost and SHAP.

The PJ-NTP-2026 batches were divided into training, validation and test subsets in a 70:15:15 ratio using stratification by influent load category, so that low-, medium- and high-strength greywater were represented in every subset. Replicate analyses of the same batch were kept in the same subset to avoid leakage between training and testing. Five-fold cross-validation within the training subset guided hyperparameter selection, the validation subset was used for model selection, and all reported surrogate metrics refer to the untouched test subset.

Table 1 reports the stage-wise quality of greywater through the NanoCircula-GW train. Influent COD of 412 mg/L fell to 96 mg/L after the bio-reactor and filter, to 38 mg/L after the photocatalytic reactor and to 27 mg/L at the membrane outlet, an overall removal of 93.4%. BOD5 decreased from 168 to 5 mg/L, surfactant concentration fell from 22.5 to 0.5 mg/L, a reduction of 97.8%, turbidity reached 2.1 NTU and E. coli was reduced from 4.2×10^4 to below 10 CFU/100 mL. The bio-reactor removes most of the biodegradable matter and part of the surfactant load, while the photocatalytic stage removes nearly all of the surfactant that survives biological treatment, lowering it from 9.8 to 1.1 mg/L, because hydroxyl and superoxide radicals generated at the g-C3N4/TiO2 interface attack the aromatic and alkyl chains that resist biological breakdown. The membrane then acts as the final barrier for particles and microorganisms and transfers part of the phosphate to the concentrate stream sent for recovery. The final effluent falls within the limits for toilet flushing and landscape irrigation, and it achieves this without the high oxidant doses that a stand-alone AOP stage would require.

Table 1: Stage-wise water quality through the NanoCircula-GW treatment train

Parameter	Influent	After bio-reactor and filter	After UV-AOP	After membrane (final)	Overall removal (%)
pH	7.4	7.2	7.0	7.1	–
Turbidity (NTU)	86	14.5	5.8	2.1	97.6
TDS (mg/L)	640	610	590	540	15.6
COD (mg/L)	412	96	38	27	93.4
BOD5 (mg/L)	168	24	8	5	97.0

© 2026 IJSRET

Parameter	Influent	After bio-reactor and filter	After UV-AOP	After membrane (final)	Overall removal (%)
LAS surfactant (mg/L)	22.5	9.8	1.1	0.5	97.8
Total nitrogen (mg/L)	38	26	22	18	52.6
Phosphate (mg/L)	9.6	7.8	7.2	3.1	67.7
E. coli (CFU/100 mL)	4.2×10^4	1.1×10^3	45	< 10	> 99.9

Figure 2 compares the COD degradation profiles of bare TiO2, bare g-C3N4 and g-C3N4/TiO2 composite plates over the irradiation period under identical conditions. The composite produces the steepest decline throughout the run, with its advantage appearing within the first minutes of irradiation and widening as the reaction progresses. Bare g-C3N4 shows the slowest response, which reflects rapid recombination of its photogenerated charges, while bare TiO2 performs better but plateaus earlier. The improved behaviour of the composite confirms that the heterojunction separates electrons and holes across the interface and sustains radical generation for longer. The figure also shows that most of the degradation is completed well before the end of the irradiation window, which allowed irradiation time, and therefore lamp energy, to be reduced in continuous operation.

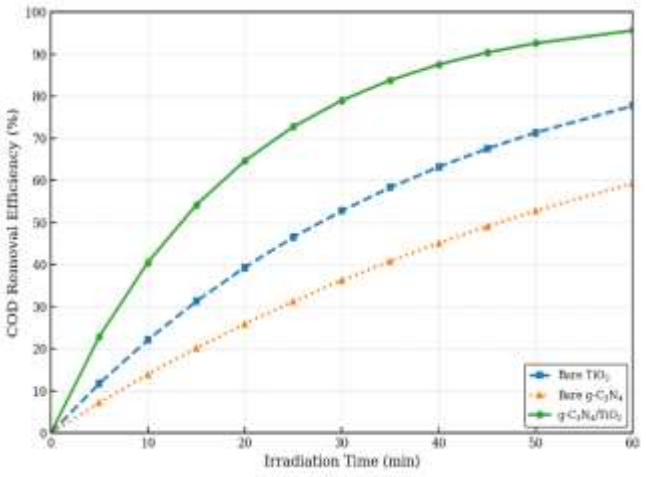

Figure 2: COD degradation profiles of bare and composite photocatalysts under UV irradiation

Table 2 summarises the membrane, nutrient-recovery and surrogate-model results. The TiO2/ZrO2-modified membrane delivered a pure water flux of 186 L/m²·h compared with 118 L/m²·h for pristine PES, and its water contact angle fell from 68° to 41°. Its flux recovery ratio after cleaning rose from 71% to 94.1%, while irreversible fouling fell from 29% to 5.9%. Greater hydrophilicity and smoother surfaces reduce the adhesion of residual surfactants and biopolymers, so fouling remains largely reversible and can be removed by hydraulic cleaning. The struvite vessel recovered 86.5% of phosphate and 74.2% of ammonium at the optimised magnesium ratio and pH. The gradient-boosting surrogate predicted COD removal with an R^2 of 0.94 and an RMSE of 2.8%, against 0.87 and 4.6% for the best baseline, the random forest; it also predicted flux decline with an R^2 of 0.91 and phosphate recovery with an R^2 of 0.89, against 0.83 and 0.81 for the best baselines. This accuracy allows the surrogate to replace many exploratory experiments whenever influent quality changes.

Table 2: Membrane, nutrient-recovery and surrogate-model performance

Parameter	Pristine PES / best baseline	NanoCircula-GW
Pure water flux (L/m²·h)	118	186
Water contact angle (°)	68	41
Flux recovery ratio (%)	71	94.1
Irreversible fouling (%)	29	5.9
Phosphate recovery as struvite (%)	–	86.5
Ammonium recovery as struvite (%)	–	74.2
Surrogate R^2 – COD removal	0.87 (random forest)	0.94
Surrogate RMSE – COD removal (%)	4.6	2.8
Surrogate R^2 – normalised flux	0.83	0.91
Surrogate R^2 – phosphate recovery	0.81	0.89

Figure 3 plots normalised permeate flux against filtration time for the pristine and modified membranes over three filtration–cleaning cycles with AOP-treated greywater. The pristine membrane loses flux quickly in every cycle and regains only part of it after cleaning, so its starting flux steps down from one cycle to the next. The modified membrane declines more gently and returns close to its initial value after each cleaning, indicating that fouling on its surface is mainly reversible. The difference becomes more pronounced with each cycle, which

© 2026 IJSRET

matters for continuous operation, where cumulative irreversible fouling determines how often chemical cleaning and membrane replacement are required. Placing the photocatalytic stage upstream also contributes, because partial oxidation of surfactants lowers the foulant load reaching the membrane.

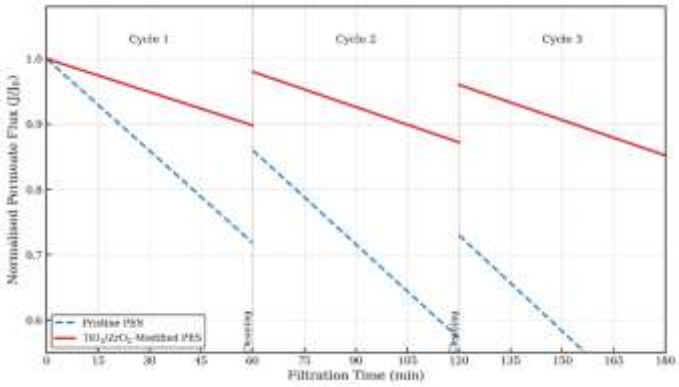

Figure 3: Normalised permeate flux of pristine and TiO2/ZrO2-modified membranes over repeated filtration–cleaning cycles

Figure 4 shows the implemented NanoCircula-GW monitoring and optimisation page. The page displays the live status of each treatment stage, stage-wise water-quality values, the predicted COD removal and flux trend generated by the surrogate, and the recommended catalyst loading, irradiation time, cleaning interval and magnesium dose. A recovery panel records struvite production for each batch, and an explanation panel lists the operating variables that most influenced the current recommendation. Operators used the page to schedule membrane cleaning and to adjust irradiation time when influent strength changed, replacing fixed manual settings with data-guided decisions.



Figure 4: Implemented NanoCircula-GW monitoring and optimisation page

Overall, the results show that the nanomaterial-enhanced stages complement the biological core rather than replacing it. The photocatalytic reactor addresses the refractory fraction, the modified membrane secures microbial and particulate quality with low fouling, and the struvite vessel turns the nutrient burden into a product. The surrogate model links these stages through operating decisions that would otherwise require repeated trials. Because the catalyst and membrane were fabricated with modest laboratory equipment and the train was operated at pilot scale, the configuration can be transferred to hostels, residential complexes and small institutions seeking both water reuse and resource recovery.

V. CONCLUSION AND FUTURE WORK

This work presented NanoCircula-GW, a circular greywater treatment train that combines biological treatment, a hydrothermally synthesised g-C3N4/TiO2 photocatalytic reactor, a TiO2/ZrO2-modified PES membrane and struvite nutrient recovery under the guidance of a gradient-boosting surrogate model. The study showed that heterojunction photocatalysis removes the surfactant and refractory organic fraction left by biological units, that nanoparticle-modified membranes sustain permeability with largely reversible fouling, and that nutrients can be recovered as a useful fertiliser within the same facility. Practically, the framework allows institutions to produce non-potable water and nutrient products while reducing chemical dosing, cleaning frequency and lamp energy. The evaluation was carried out at pilot scale on campus greywater, and longer campaigns across seasons will further establish catalyst and membrane durability. Future work will examine solar-driven operation, additional emerging contaminants and integration with real-time sensing and aquifer recharge.

REFERENCES

1. Budeli, P., & Sibali, L. L. (2025). Greywater reuse: Contaminant profile, health implications, and sustainable solutions. *International Journal of Environmental Research and Public Health, 22*(5), 740. https://doi.org/10.3390/ijerph22050740
2. Mohan, S., Manthapuri, V., & Chitthaluri, S. (2024). Assessing factors influencing greywater characteristics around the world: A qualitative and quantitative approach with a short-review on greywater treatment technologies. *Discover Water, 4*, 37. https://doi.org/10.1007/s43832-024-00094-w
3. Nourredine, H., & Barjenbruch, M. (2024). Graywater treatment efficiency and nutrient removal using moving

© 2026 IJSRET

bed biofilm reactor (MBBR) systems: A comprehensive review. *Water, 16*(16), 2330. https://doi.org/10.3390/w16162330
4. Kruopienė, J., & Smol, M. (2024). Resource recovery monitoring and circular economy model in wastewater. *Water, 16*(18), 2557. https://doi.org/10.3390/w16182557
5. Ruffino, B., & Campo, G. (2025). Circular water resources integrating sustainability and innovation in wastewater and water management. *Resources, 15*(1), 4. https://doi.org/10.3390/resources15010004
6. Hamidi, M. N. (2025). Membrane bioreactor technology for greywater treatment: A review. *Separation and Purification Technology, 361*, 131451. https://doi.org/10.1016/j.seppur.2025.131451
7. Ittisupornrat, S., Namyuang, C., Phetrak, A., Sriromreun, P., & Theepharaksapan, S. (2025). Microplastic contamination and removal efficiency in greywater treatment using a membrane bioreactor. *Frontiers in Microbiology, 16*, 1519230. https://doi.org/10.3389/fmicb.2025.1519230
8. Patil, Y., Priya, B. S. L., Sonawane, S. H., & Shyam, P. (2023). Comparative performance of Fenton and cavitation assisted Fenton techniques for effective treatment of greywater. *Journal of Environmental Chemical Engineering, 11*(5), 110667. https://doi.org/10.1016/j.jece.2023.110667
9. Mackey, E., Hofmann, R., Festger, A., Vanyo, C., Moore, N., Chen, T., Wang, C., Taylor-Edmonds, L., & Andrews, S. A. (2023). UV-chlorine advanced oxidation for potable water reuse: A review of the current state of the art and research needs. *Water Research X, 19*, 100183. https://doi.org/10.1016/j.wroa.2023.100183
10. Guo, B., Uzzaman, M., Furukawa, M., Tateishi, I., Katsumata, H., & Kaneco, S. (2024). Photocatalytic purification of Orange-II-dye-polluted wastewater using TiO2-modified g-C3N4 composite. *C, 10*(4), 103. https://doi.org/10.3390/c10040103
11. Liu, R., Li, M., Chen, J., Yin, Y., Zhao, W., Gong, Z., Jin, H., & Liu, Z. (2024). Enhanced photocatalytic degradation of tetracycline by magnetically separable g-C3N4-doped magnetite@titanium dioxide heterostructured photocatalyst. *Water, 16*(10), 1372. https://doi.org/10.3390/w16101372
12. Nhlengethwa, S. T., Tshangana, C. S., Mamba, B. B., & Muleja, A. A. (2024). The application of TiO2/ZrO2-modified nanocomposite PES membrane for improved permeability of textile dye in water. *Membranes, 14*(10), 222. https://doi.org/10.3390/membranes14100222
13. Güneş-Durak, S., Acarer-Arat, S., Tüfekci, M., Pir, İ., Üstkaya, Z., Öz, N., & Tüfekci, N. (2024). Mechanical enhancement and water treatment efficiency of nanocomposite PES membranes: A study on Akçay Dam water filtration application. *ACS Omega, 9*(29), 31556–31568. https://doi.org/10.1021/acsomega.4c01410
14. Abuwatfa, W. H., AlSawaftah, N., Darwish, N., Pitt, W. G., & Husseini, G. A. (2023). A review on membrane fouling prediction using artificial neural networks (ANNs). *Membranes, 13*(7), 685. https://doi.org/10.3390/membranes13070685
15. Cairone, S., Hasan, S. W., Choo, K.-H., Li, C.-W., Zorpas, A. A., Ksibi, M., Zarra, T., Belgiorno, V., & Naddeo, V. (2024). Enhancing membrane fouling control in wastewater treatment processes through artificial intelligence modeling: Research progress and future perspectives. *Euro-Mediterranean Journal for Environmental Integration, 9*(4), 1887–1905. https://doi.org/10.1007/s41207-024-00659-0
16. K C, A., Sankar Rao, C., & Nair, V. (2024). Combination of ensemble machine learning models in photocatalytic studies using nano TiO2 – lignin based biochar. *Chemosphere, 352*, 141326. https://doi.org/10.1016/j.chemosphere.2024.141326
17. Gnanaprakasam, A., Thirumarimurugan, M., & Shanmathi, N. (2024). Machine learning, a powerful tool for the prediction of BiVO4 nanoparticles efficiency in photocatalytic degradation of organic dyes. *Journal of Environmental Science and Health, Part A, 59*(1), 15–24. https://doi.org/10.1080/10934529.2024.2319510
18. Guan, Q., Li, Y., Zhong, Y., Liu, W., Zhang, J., Yu, X., Ou, R., & Zeng, G. (2023). A review of struvite crystallization for nutrient source recovery from wastewater. *Journal of Environmental Management, 344*, 118383. https://doi.org/10.1016/j.jenvman.2023.118383
19. Nadagouda, M. N., Varshney, G., Varshney, V., & Hejase, C. A. (2024). Recent advances in technologies for phosphate removal and recovery: A review. *ACS Environmental Au, 4*(6), 271–291. https://doi.org/10.1021/acsenvironau.3c00069
20. Yan, Y., Kallikazarou, N., Nisiforou, O. A., Shang, Q., Fu, D., Antoniou, M. G., & Fotidis, I. A. (2025). Phosphorus recovery through struvite crystallization from real wastewater: Bridging gaps from lab to market. *Bioresource Technology*, 132408. https://doi.org/10.1016/j.biortech.2025.132408

© 2026 IJSRET